Supporting Information: Energetic optimization of thermochemical air separation for the production of sustainable nitrogen

1 Thermodynamic properties

Thermodynamic properties of the materials investigated are summarized in table 1. The values of $Ca_{1\text{-}x}Sr_xMnO_{3\text{-}\delta}$ are extracted from[1] with a linear approximation. The original data was collected via the van't Hoff approach of thermogravimetric measurements.

Table 1 Thermodynamic properties of the materials investigated.

Material	Δh°_δ [$kJmol^{-1}$]	Δs°_δ [$Jmol^{-1}K^{-1}$]	a [-]	extracted from
$SrFeO_{3\text{-}\delta}$	74	47	1.07	[2]
$Sr_{0.8}Ca_{0.2}FeO_{3\text{-}\delta}$	57.5	-	-	[3]
$CaMnO_{3\text{-}\delta}$	180	108	1	[1]
$Ca_{0.9}Sr_{0.1}MnO_{3\text{-}\delta}$	168	100	1	[1]
$Ca_{0.8}Sr_{0.2}MnO_{3\text{-}\delta}$	157	92	1	[1]
$Ca_{0.7}Sr_{0.3}MnO_{3\text{-}\delta}$	146	84	1	[1]
$Ca_{0.6}Sr_{0.4}MnO_{3\text{-}\delta}$	135	76	1	[1]

2 Calculation of pressure drop Δp

The pressure drop Δp during oxidation and reduction at 1 bar is calculated based on the Ergun equation[4]. The necessary input values are listed in the following:

$$\text{length of the packed bed } \Delta L : 500\,\text{mm}$$
$$\text{fluid velocity in the empty pipe } v : 0.422\,\frac{\text{m}}{\text{s}}$$
$$\text{porosity of the filling } \psi : 0.4$$
$$\text{Sauter particle diameter } d : 1.5\,\text{mm}$$

The temperature and pressure dependent dynamic viscosity and fluid density are summarized in table 2 and 3. These values are calculated based on the material properties of air extracted from[5].

Table 2 Dynamic viscosity η in $\frac{\mathrm{kg}}{\mathrm{ms}}$ calculated for the applied temperatures and pressures during oxidation and reduction.

		Temperature [K]					
		623	873	973	1023	1173	1223
pressure [bar]	1	316.5	398.0	427.9	442.4	484.6	498.4
	2	316.8		427.7	442.1		
	3	316.8		427.7	442.1		
	4	316.8		427.7	442.1		
	5	317.1		427.6	441.9		

Table 3 Fluid density of air in $\frac{kg}{m^3}$ calculated for the applied temperatures and pressures during oxidation and reduction.

		Temperature [K]					
		623	873	973	1023	1173	1223
pressure [bar]	1	0.56	0.398	0.358	0.341	0.3	0.288
	2	1.092		0.728	0.702		
	3	1.626		1.097	1.060		
	4	2.161		1.465	1.418		
	5	2.691		1.873	1.782		

The resulting pressure drop Δp is listed in the following table.

Table 4 Pressure drop Δp in bar. Calculated for the applied temperatures and pressures during oxidation and reduction.

		Temperature [K]					
		623	873	973	1023	1173	1223
pressure [bar]	1	0.0143	0.0248	0.0295	0.0319	0.0395	0.0423
	2	0.0073		0.0145	0.0155		
	3	0.0049		0.0096	0.0103		
	4	0.0037		0.0072	0.0077		
	5	0.0030		0.0057	0.0060		

3 Material composition of $SrFeO_{3-\delta}$ granules

The material composition of the $SrFeO_{3-\delta}$ granules was studied with powder X-ray diffraction (XRD) using a *D8-Advance (A25)* instrument from *Bruker* with a cobalt

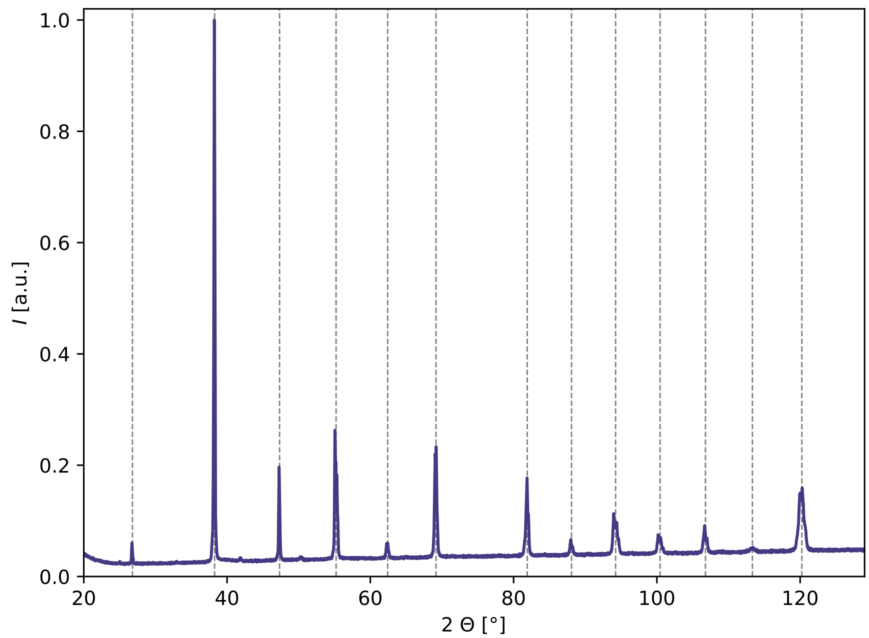

Figure 1 XRD-pattern of the $SrFeO_{3\text{-}\delta}$ granules. This patter was measured with a cobalt anode. The vertical lines indicate the main peaks of the structure with which this pattern was identified. They refer to PDF 01-081-9514 of the database *PDF 2 - Release 2019 RDB* of the *International Center for Diffraction Data (ICCD)*.

anode and a *Lynxe-EyeXET-Detector* (fig.1).

The figure 1 shows that the granules prepared are $SrFeO_{3\text{-}\delta}$ granules without major side phases. The vertical lines indicate the peak positions of the PDF 01-081-9514 of the database *PDF 2 - Release 2019 RDB* of the *International Center for Diffraction Data (ICCD)*.

4 Additional graphs for parametric study

The figures 2 and 3 display both graphs of fig. 6d in the main manuscript separately.

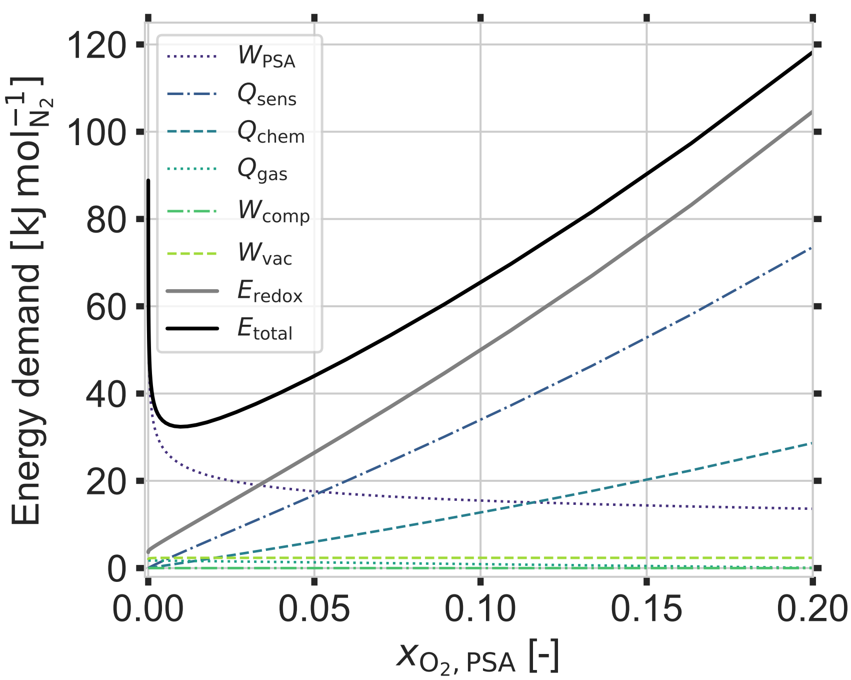

Figure 2 Variation of the PSA output oxygen x_{O_2} mole fraction and thus of the oxygen partial pressure during oxidation for $Sr_{0.8}Ca_{0.2}FeO_{3\text{-}\delta}$.

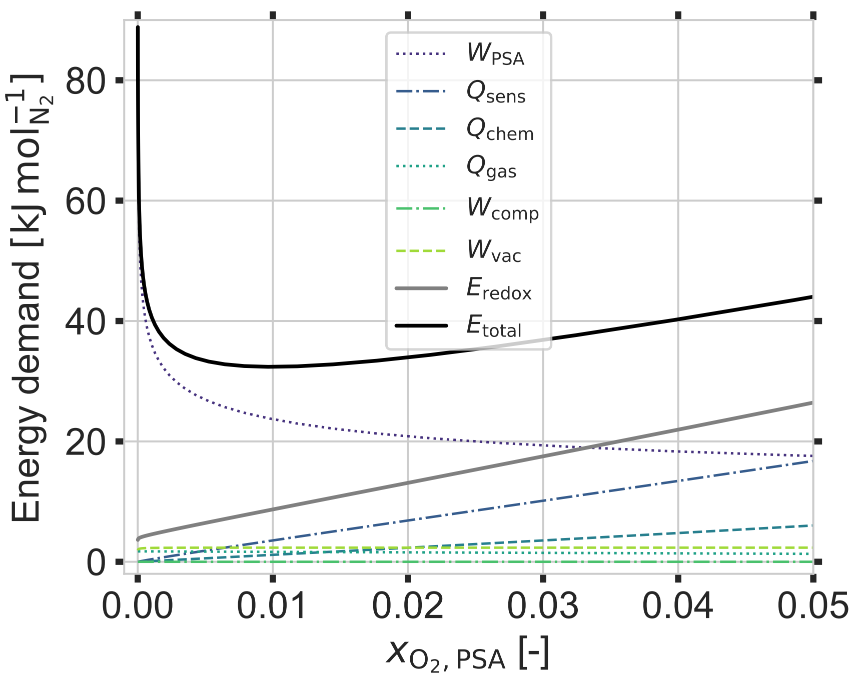

Figure 3 Extract from fig. 2.

References

[1] L. Klaas, B. Bulfin, D. Kriechbaumer, M. Roeb and C. Sattler, *Physical Chemistry Chemical Physics*, 2023, **25**, 9188–9197.

[2] J. Vieten, B. Bulfin, D. E. Starr, A. Hariki, F. M. F. de Groot, A. Azarpira, C. Zachäus, M. Hävecker, K. Skorupska, N. Knoblauch, M. Schmücker, M. Roeb and C. Sattler, *Energy Technology*, 2018, **7**, 131–139.

[3] S. Capstick, B. Bulfin, J. Naik, M. Gigantino and A. Steinfeld, *Chemical Engineering Journal*, 2023, **452**, 139289.

[4] S. Ergun, *Chemical Engineering Progress*, 1952, **48**, 89–94.

[5] V. D. I.-G. V. und Chemieingenieurwesen (GVC), *VDI-Wärmeatlas (VDI-Buch)*, Springer, 2005, p. 1500.